

HOSTED BY



ELSEVIER

Contents lists available at ScienceDirect

Engineering Science and Technology, an International Journal

journal homepage: <http://www.elsevier.com/locate/jestch>

Full length article

Geometrically nonlinear free vibration analysis of axially functionally graded taper beams

Saurabh Kumar ^a, Anirban Mitra ^{b,*}, Haraprasad Roy ^a^a Mechanical Engineering Department, National Institute of Technology, Rourkela 769008, Odisha, India^b Department of Mechanical Engineering, Jadavpur University, Kolkata 700032, India

ARTICLE INFO

Article history:

Received 12 January 2015

Received in revised form

27 March 2015

Accepted 2 April 2015

Available online xxx

Keywords:

Large amplitude

Energy principles

Geometric nonlinearity

Backbone curve

ABSTRACT

Large amplitude free vibration analysis is carried out on axially functionally graded (AFG) tapered slender beams under different boundary conditions. The problem is addressed in two parts. First the static problem corresponding to a uniform transverse loading is solved through an iterative scheme using a relaxation parameter and later on the subsequent dynamic problem is solved as a standard eigenvalue problem on the basis of known static displacement field. The mathematical formulation of the static problem is based on the principle of minimum total potential energy, whereas Hamilton's principle has been applied for the dynamic analysis. To account for the geometric non-linearity arising due to large deflection, nonlinear strain displacement relations are considered. The dynamic behaviour has been presented in the form of backbone curves in a dimensionless frequency–amplitude plane. The results are successfully validated with the previously published results.

Copyright © 2015, Karabuk University. Production and hosting by Elsevier B.V. This is an open access article under the CC BY-NC-ND license (<http://creativecommons.org/licenses/by-nc-nd/4.0/>).

1. Introduction

Non-uniform beams with variable cross-section provide a suitable distribution of mass and strength for engineering structures. These structural elements are commonly used in various engineering applications, such as, gas turbines, wind turbines, helicopter rotor blades, ship propellers, robot arms, space and marine structures etc. [12]. Their wide-spread usage in various advanced branches of civil, mechanical and construction industries is due to their ability to cater to different structural requirements. Hence, prediction and determination of dynamic behaviour of these components have been an area of great interest among researchers.

Functionally graded materials (FGMs) are new and advanced class of inhomogeneous composites, which are obtained by combination of two or more constituent materials, mixed continuously and functionally according to a given volume fraction. As a result, material properties become a function of spatial position and a continuous variation from one surface to another can be achieved. In this respect, FGMs are advantageous over contemporary laminated composites as property variation is continuous and thus

eliminate stress concentration [30]. Whereas, laminated composites suffer from the disadvantage of discontinuity at the layer interface and subsequent stress concentration. In the modern context, FGMs find extensive application in aerospace, civil and mechanical engineering fields [43], especially, where, unevenly distributed thermal, chemical or mechanical loads are present.

The variation of material properties in functionally graded (FG) beams may be oriented in transverse (thickness) direction or longitudinal/axial (length) direction or both. An exhaustive literature review of the relevant domain reveals that majority of the studies are concentrated on free vibration analysis of FG beams with material property variation along the depth of the beam. In case of a free vibration study of a structure the main objective is to determine the natural frequencies corresponding to various modes of vibration of the system. Several different techniques and methodologies have been adopted for this purpose by different researchers [6,44] derived the governing equations using Hamilton's principle while employing different higher order shear deformation theories and obtained the solution to these equations using Navier solution method. Analysis of free vibration of FG beams was also carried out by [23,41,42]; who used different techniques to solve the governing equations obtained from application of Hamilton's principle. Nguyen et al. [30] introduced a method involving first-order shear deformation beam theory where the improved shear stiffness matrix was derived from the in-plane stress and equilibrium equation.

* Corresponding author. Tel./fax: +91 33 2414 6890.

E-mail address: samik893@gmail.com (A. Mitra).

Peer review under responsibility of Karabuk University.

<http://dx.doi.org/10.1016/j.jestch.2015.04.003>

2215-0986/Copyright © 2015, Karabuk University. Production and hosting by Elsevier B.V. This is an open access article under the CC BY-NC-ND license (<http://creativecommons.org/licenses/by-nc-nd/4.0/>).

Nomenclature

A_0	cross-sectional area of the beam at the root
b	width of the beam
c_i	unknown coefficients for static analysis
d_i	unknown coefficients for dynamic analysis
E_0	elastic modulus of the beam material at the root
$\{f\}$	load vector
I_0	moment of inertia of the beam at the root
$[K]$	stiffness matrix
$[K_s]$	static stiffness matrix
L	length of the beam
$[M]$	mass matrix
nw, nu	number of constituent functions for w and u respectively
ng	number of Gauss points
p	magnitude of uniformly distributed load
t_0	thickness of the beam at the root

T	kinetic energy of the system
u	displacement field in x -axis
U	strain energy stored in the system
V	potential energy of the external forces
w	displacement field in z -axis
w_{max}	maximum deflection of the beam
α	taper parameter
δ	variational operator
$\varepsilon_x^b, \varepsilon_x^s$	axial strains due to bending and stretching respectively
ρ_0	density of the beam material at the root
τ	time coordinate
ω_1	first natural frequency
ω_{nl}	nonlinear frequency parameters
ξ	normalized axial coordinate
π	total potential energy of the system
ψ_i	set of orthogonal functions for u
ϕ_i	set of orthogonal functions for w

It is found that finite element techniques are quite popular in analyzing the dynamics of FG beams. Chakraborty et al. [7] developed a new beam element also based on the first order shear deformation theory to study the free vibration of FG beams. Hemmatnezhad et al. [15] investigated the nonlinear behavior of FG beams using finite element formulation. Von Karman type nonlinear equations along with Timoshenko beam theory were used for the analysis. Piovan and Sampaio [32] studied the free vibration of axially moving thin-walled beam with annular cross-section using finite element method. Ke et al. [21] studied the nonlinear free vibration of FG beams using Galerkin's method. The nonlinear equations were based on Von Karman geometric nonlinearity and the governing equations were solved using direct numerical integration method and Runge-Kutta method.

The Ritz method along with an improved third order shear deformation theory was used by Ref. [45]. Li [24] adopted a new unified approach where a single fourth-order governing partial differential equation was derived. The analysis by [33] was based on classical and first order shear deformation theories where the governing equations were obtained using Rayleigh-Ritz method. Simsek [38] dealt with the classical, first and higher shear deformation theories and derived the equations of motion employing Lagrange's equations. Giunta et al. [11] worked with several axiomatic refined theories and derived the governing differential equations by variationally imposing the equilibrium through the principle of virtual displacements. Murin et al. [29] derived fourth-order differential equation for the FG beam and used linear beam theory to establish equilibrium and kinetic beam equations. Simsek and Kocaturk [39] used Lagrange's equations along with Euler-Bernoulli beam theory to study the free vibration behavior of FG beams under the action of concentrated moving loads. A total Lagrangian formulation was used by [1] to investigate the effects of geometric nonlinearity on the static and dynamic response of FG beams. Lu and Chen [26] obtained semi-analytical solutions for the free vibration of orthotropic FG beams using a hybrid state-space differential quadrature method along with an approximate laminate model. Kapuria et al. [20] presented a theoretical model and its experimental validation for the free vibration of a layered FG beam. Some research works are also available on the effect of nonlinear elastic foundations on free vibration behavior of FG beams [10,19,31,47]. The governing equations were based on Euler-Bernoulli beam theory and solved using Galerkin's method and He's variational iteration method.

A few researchers have concentrated on the free vibration of FG beams where the material property variation is along the length of the beam. Simsek et al. [40] derived the equation of motion by using Lagrange's equations and Newmark method was employed to find the dynamic responses of AFG beam. Shahba et al. [35–37] and Shahba and Rajasekaran [34] studied the free vibration and stability analysis of Euler-Bernoulli and Timoshenko beams through finite element approach and various numerical analysis methods. Alshorbagy et al. [4] employed numerical FEM and Euler-Bernoulli beam theory to investigate the dynamic characteristics of FG beams. Huang et al. [18] presented a new approach for investigating the vibration behaviors of non-uniform AFG Timoshenko beams by changing the coupled governing equations to a single governing equation by introducing an auxiliary function. Huang and Li [16,17] studied the dynamic and buckling behavior of AFG tapered beams by reducing the corresponding governing differential equation to Fredholm integral equations. Aydogdu [5], Elishakoff et al. [9] and Wu et al. [46] investigated the free vibrations of AFG tapered beams using the semi inverse method. Mazzei and Scott [27] studied stability and vibration of AFG tapered shafts loaded by axial compressive forces. Li et al. [25] derived the characteristic equations in closed form for exponentially graded beams with various boundary conditions. Kein [22] investigated the large displacement response of tapered AFG cantilever beams by finite element method. Hein and Feklistova [14] studied the vibrations of non-uniform FG beams with various boundary conditions using the Euler-Bernoulli theory and Haar wavelets. Akgoz and Civalek [3] performed vibration response analysis of AFG tapered micro beams with Euler-Bernoulli beam theory and modified couple stress theory, by utilizing Rayleigh-Ritz solution method. The authors [2] also investigated buckling problem of linearly tapered cantilever micro-columns of rectangular and circular cross-section on the basis of modified strain gradient elasticity theory.

Literature review reveals that a substantial amount of research work is focused on the field of free vibration study of depth-wise functionally graded beams, while relatively fewer research studies are available for AFG beams. Works on large amplitude free vibration, specifically variation of loaded natural frequencies with external transverse loading of AFG taper beams is limited. It should be pointed out that a vast majority of research papers deal with a particular type (Linear) of taper profile, while the emphasis remains on developing new methods to determine the natural frequencies of the system. Hence, the present study is taken up with

the objective of analyzing the large amplitude free vibration problem of axially functionally graded (AFG) tapered beams with different taper profiles. Variation of material properties (elastic modulus and density) along the length of the beam is considered according to different functions. Effect of variation of system geometry (taper parameter) on the dynamic behaviour is also studied. The large amplitude free vibration behavior is presented as backbone curves in non-dimensional amplitude-frequency plane, where, variation of natural frequency with the maximum amplitude of deflection yields the backbone curve of the system. The nature of change in the mode shape with increase in vibration amplitude is also investigated.

2. Mathematical formulation

An axially functionally graded non-uniform beam of length L with variable cross-sectional dimensions ($b \times t(x)$) is shown in Fig. 1 along with the coordinate system for the present analysis. The modulus of elasticity $E(x)$ and mass density $\rho(x)$ of the beam shown in figure vary with respect to the longitudinal direction along the x -axis. It is to be noted that the computations are carried out in normalized coordinate ξ , which is given by, $\xi = x/L$. Although the figure shows only varying thickness ($t(x)$) with constant width, the formulation is capable of handling varying width as well. Effects of shear deformation and rotary inertia have been neglected as the cross-sectional dimensions are assumed to be considerably smaller than the length of the beam.

The present semi-analytical formulation is displacement based and employs appropriate energy approach to arrive at the governing equations of the system. According to [8]; large amplitude vibration analysis of a nonlinear system may be considered equivalent to its free vibration analysis, under static load producing same magnitude of large amplitude deflection. The system is assumed to execute small-amplitude vibration about the statically deflected equilibrium configuration as opposed to large-amplitude vibration about its undeformed equilibrium position. The magnitude of large amplitude vibration is equal to the static large displacement inflicted on the system under loading. Hence, the present large amplitude free vibration analysis is performed in two steps. Determination of large amplitude vibration frequencies (loaded natural frequencies) involves solving the static displacement of the AFG beam through an iterative scheme in the first part. Subsequently dynamic study is taken up as a standard eigenvalue problem on the basis of known static displacement field. As the dynamic problem is solved on the basis of the solution of the static displacement field, the effect of statically imposed large amplitude of vibration is incorporated into the dynamic system [28]. Both the static and dynamic problems are formulated on the basis of variational form of energy principle. Nonlinear strain-displacement relations are taken into account in order to incorporate geometric nonlinearity.

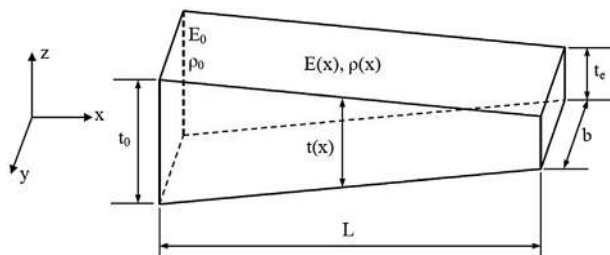


Fig. 1. Axially FG tapered beam with variation of material properties and geometrical dimensions.

2.1. Static analysis

As already stated, the present analysis is based on the assumption of the beam being slender i.e. the thickness of the beam is small compared to its length, such that the effect of shear deformation and rotary inertia may be neglected. The governing set of equations for the static analysis is derived through the principle of minimum total potential energy, which states that,

$$\delta(\pi) = 0, \tag{1}$$

where,

$$\pi = U + V.$$

π = Total potential energy of the system,

U = Total strain energy stored in the system,

V = Work function or potential of the external forces,

δ = Variational operator.

In the case of large displacement analysis of beams, both bending and stretching effects are taken into consideration. Therefore, total strain energy stored in the beam is given by:

$$U = U_b + U_m \tag{2a}$$

where,

$$U_b = \text{strain energy stored due to bending} = \frac{1}{2} \int_{vol} E(x) (\epsilon_x^b)^2 dv \tag{2b}$$

$$U_m = \text{strain energy stored due to stretching} = \frac{1}{2} \int_{vol} E(x) (\epsilon_x^s)^2 dv \tag{2c}$$

ϵ_x^b and ϵ_x^s are axial strains due to bending and stretching respectively. The expressions for axial strain due to bending at a distance z from the neutral axis and axial strain due to stretching of neutral axis are respectively given by: $\epsilon_x^b = -z \frac{d^2w}{dx^2}$ and $\epsilon_x^s = \frac{du}{dx} + \frac{1}{2} \left(\frac{dw}{dx} \right)^2$.

Substituting these strain expressions into Equation (2), the total strain energy stored in the beam turns out to be:

$$U = \frac{1}{2} \int_0^L \left(\frac{d^2w}{dx^2} \right)^2 E(x) I(x) dx + \frac{1}{2} \int_0^L \left[\left(\frac{du}{dx} \right)^2 + \frac{1}{4} \left(\frac{dw}{dx} \right)^4 + \left(\frac{dw}{dx} \right)^2 \left(\frac{du}{dx} \right) \right] E(x) A(x) dx \tag{3}$$

The work potential of the external load calculated corresponding to an externally applied uniformly distributed load of intensity p is given by:

$$V = \int_0^L p(x) w dx \tag{4}$$

Transverse loading patterns other than uniformly distributed load (for example, point load, triangular or hat distribution etc.) can also be accounted for in the present methodology, as long as they are expressible mathematically by analytical or numerical

Table 1

Base functions for assumed displacement fields (w, u).

Flexural Boundary condition	$\phi_i(\xi)$
CC	$\{\xi(1-\xi)\}^2$
CF	$\xi^2(\xi^2-4\xi+6)$
In-plane Boundary condition	$\psi_i(\xi)$
Immovable	$\xi(1-\xi)$

functions. Substituting Equations (3) and (4) in Equation (1), the following expression is obtained,

$$\delta \left[\frac{1}{2} \int_0^L \left(\frac{d^2w}{dx^2} \right)^2 E(x)I(x)dx + \frac{1}{2} \int_0^L \left\{ \left(\frac{du}{dx} \right)^2 + \frac{1}{4} \left(\frac{dw}{dx} \right)^4 + \left(\frac{dw}{dx} \right)^2 \left(\frac{du}{dx} \right) \right\} E(x)A(x)dx + \int_0^L p(x)w dx \right] = 0 \tag{5}$$

Using normalised coordinate ($\xi = x/L$), the above expression can be rewritten as follows.

$$\delta \left[\frac{1}{2} \int_0^1 \frac{1}{L^3} \left(\frac{d^2w}{d\xi^2} \right)^2 E(\xi)I(\xi)d\xi + \frac{1}{2} \int_0^1 \left\{ \frac{1}{L} \left(\frac{du}{d\xi} \right)^2 + \frac{1}{4L^3} \left(\frac{dw}{d\xi} \right)^4 + \frac{1}{L^2} \left(\frac{dw}{d\xi} \right)^2 \left(\frac{du}{d\xi} \right) \right\} E(\xi)A(\xi)d\xi + \int_0^1 p(\xi)wLd\xi \right] = 0 \tag{6}$$

After applying the variational operator the above equation becomes,

$$\frac{1}{L^3} \int_0^1 \left(\frac{d^2w}{d\xi^2} \right) \delta \left(\frac{d^2w}{d\xi^2} \right) E(\xi)I(\xi)d\xi + \left[\frac{1}{L} \int_0^1 \left(\frac{du}{d\xi} \right) \delta \left(\frac{du}{d\xi} \right) + \frac{1}{2L^3} \int_0^1 \left(\frac{dw}{d\xi} \right)^3 \delta \left(\frac{dw}{d\xi} \right) + \frac{1}{L^2} \int_0^1 \left(\frac{du}{d\xi} \right) \left(\frac{dw}{d\xi} \right) \delta \left(\frac{dw}{d\xi} \right) + \frac{1}{2L^2} \int_0^1 \left(\frac{dw}{d\xi} \right)^2 \delta \left(\frac{du}{d\xi} \right) \right] E(\xi)A(\xi)d\xi + \int_0^1 p(\xi)\delta wLd\xi = 0 \tag{7}$$

Here, w and u are transverse and in-plane displacements of the beam, respectively. In the present analysis these two displacements

(w and u) are the basic unknown variables. These approximate displacement fields, w and u , are expressed by linear combinations of unknown coefficients (c_i) and orthogonal admissible functions (ϕ and ψ) as follows,

$$w(\xi) = \sum_{i=1}^{nw} c_i \phi_i(\xi) \text{ and } u(\xi) = \sum_{i=nw+1}^{nw+nu} c_i \psi_i(\xi) \tag{8}$$

In above expressions, nw and nu are number of functions for w and u , respectively. The functions $\phi_i(\xi)$ are associated with displacements due to bending, whereas $\psi_i(\xi)$ describe stretching of the neutral plane of the beam. These admissible functions (ϕ and ψ) are continuous and differentiable within the domain and also satisfy the boundary conditions of the system. It is also well known that in applying the assumed series solution for the assumed field proper choice of the functions is very important. Satisfactory result can be obtained when the admissible functions come from a set of orthogonal functions. The basis functions for these orthogonal sets of functions are selected in such way that they satisfy the necessary geometric boundary conditions of the beam. The 1-D base functions for transverse displacement (w) are taken as the beam deflection functions, derived from static deflection shape of the beam, corresponding to the boundary condition of the system. The starting functions for stretching of the beam (u) come from the in-plane boundary conditions, and zero displacement is assumed at the boundaries, i.e., $u = 0$ at $\xi = 0,1$. Gram-Schmidt orthogonalization procedure is used to generate appropriate sets of higher order coordinate functions from the selected admissible start functions. Objective of the present numerical implementation of Gram Schmidt orthogonalization scheme is to determine a set of orthogonal functions (admissible) in the interval $0 \leq \xi \leq 1$, provided the first function, $\phi_1(\xi)$, of the set is known (chosen satisfying boundary conditions).

$$\phi_2(\xi) = (\xi - B_1) \phi_1(\xi) \tag{9a}$$

$$\phi_k(\xi) = (\xi - B_k) \phi_{k-1}(\xi) - C_k \phi_{k-2}(\xi), \text{ where,}$$

$$B_k = \frac{\int_0^1 \xi \beta(\xi) \phi_{k-1}^2(\xi) d\xi}{\int_0^1 \beta(\xi) \phi_{k-1}^2(\xi) d\xi} \tag{9b}$$

$$C_k = \frac{\int_0^1 \xi \beta(\xi) \phi_{k-1}(\xi) \phi_{k-2}(\xi) d\xi}{\int_0^1 \beta(\xi) \phi_{k-2}^2(\xi) d\xi}$$

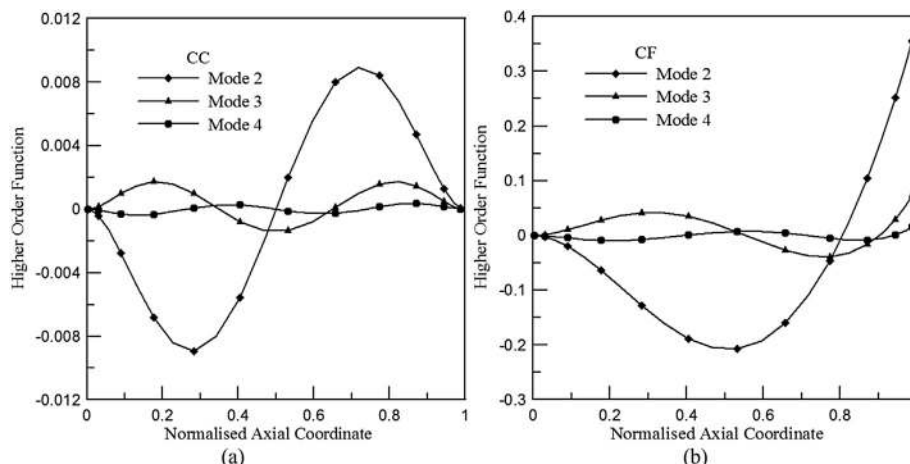


Fig. 2. Graphical representation of higher order one dimensional (1-D) beam functions: (a) CC, and (b) CF.

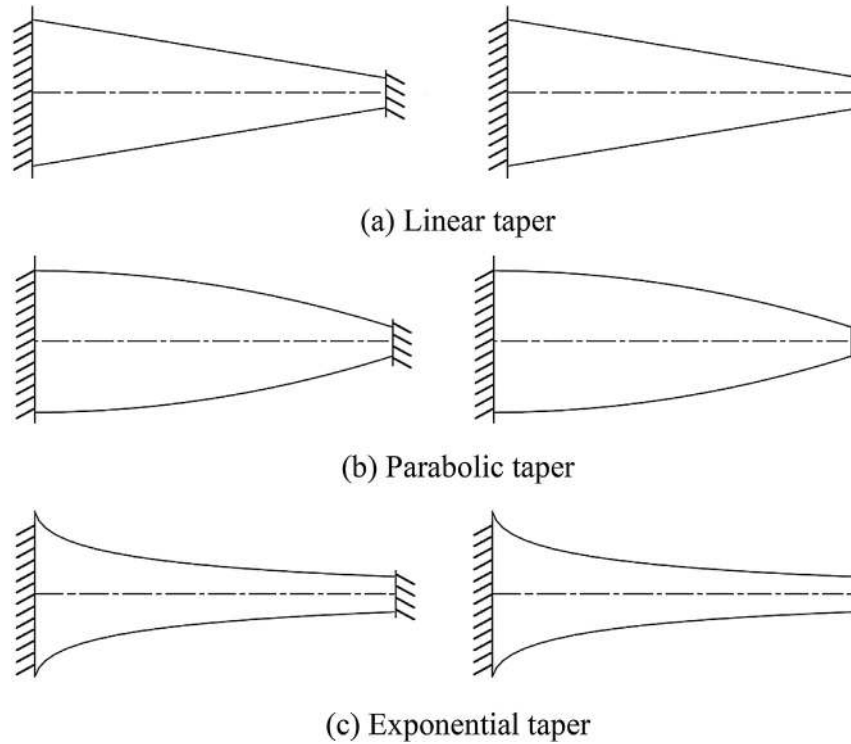


Fig. 3. Schematic representation of taper profile and boundary conditions of AFG beams.

with $\beta(\xi)$ being the weight function. The set of function $\phi_k(\xi)$ satisfies the orthogonality condition given by,

$$\int_0^1 \beta(\xi) \phi_k(\xi) \phi_l(\xi) d\xi = \begin{cases} 0 & \text{if } k \neq l \\ 1 & \text{if } k = l \end{cases} \quad (9c)$$

For the present work, the weight function is chosen as unity. For the convenience of the numerical scheme, all the functions are defined numerically at some suitably selected Gauss points.

Substituting the expressions of appropriate displacement fields from Equation (8) in Equation (7) gives the governing set of equations for static deflection of the beam. The governing set of equations in matrix form is given as,

$$[K_s]\{c\} = \{f\}, \quad (10)$$

where, $[K_s]$ is the stiffness matrix corresponding to static analysis, $\{f\}$ is the force vector for transverse static external load and $\{c\}$ is a vector of unknown coefficients. The forms of stiffness matrix and load vector are given as follows.

$[K_s] = \begin{bmatrix} K_{11} & K_{12} \\ K_{21} & K_{22} \end{bmatrix}$ and $\{f\} = \{f_{11} \ f_{12}\}^T$ The elements of $[K_s]$ and $\{f\}$ are:

Table 2
Values of taper parameter for different taper patterns.

Taper Pattern	$\alpha = 0.0$	$\alpha = 0.2$	$\alpha = 0.4$	$\alpha = 0.6$
Linear taper				
Parabolic taper				
Exponential taper		0.223144	0.510826	0.916291

$$[K_{11}] = \frac{1}{L^3} \sum_{j=1}^{nw} \sum_{i=1}^{nw} \int_0^1 \frac{d^2 \phi_i}{d\xi^2} \frac{d^2 \phi_j}{d\xi^2} E(\xi) I(\xi) d\xi$$

$$+ \frac{1}{2L^3} \sum_{j=1}^{nw} \sum_{i=1}^{nw} \int_0^1 \left(\sum_{i=1}^{nw} c_i \frac{d\phi_i}{d\xi} \right)^2 \frac{d\phi_i}{d\xi} \frac{d\phi_j}{d\xi} E(\xi) A(\xi) d\xi$$

$$+ \frac{1}{L^2} \sum_{j=1}^{nw} \sum_{i=1}^{nw} \int_0^1 \left(\sum_{i=nw+1}^{nw+nu} c_i \frac{d\psi_{i-nw}}{d\xi} \right)^2 \frac{d\phi_i}{d\xi} \frac{d\phi_j}{d\xi} E(\xi) A(\xi) d\xi,$$

Table 3

Non-dimensional transverse frequencies ($\omega = \mu L^2 \sqrt{\rho A_0/E_0 I_0}$) for linearly tapered AFG beam ($E(\xi) = E_0(1 + \xi)$, $\rho(\xi) = \rho_0(1 + \xi + \xi^2)$).

α	Research work by	Vibration frequencies			
		CC		CF	
		ω_1	ω_2	ω_1	ω_2
0.0	Present	20.3949	56.3144	2.4254	18.6034
	[34]	20.4721	56.5481	2.4255	18.6041
	% error	0.3770	0.4132	0.0041	0.0037
0.2	Present	18.1479	50.2697	2.5053	17.3820
	[34]	18.2169	50.4792	2.5051	17.3801
	% error	0.3787	0.4150	0.0079	0.0109
0.4	Present	15.7673	43.8395	2.6162	16.0749
	[34]	15.8281	44.0236	2.6155	16.0705
	% error	0.3841	0.4182	0.0267	0.0273
0.6	Present	13.1765	36.8059	2.7846	14.6579
	[34]	13.2291	36.9636	2.7835	14.6508
	% error	0.3976	0.4266	0.0395	0.0484
0.8	Present	10.1766	28.6035	3.0882	13.1256
	[34]	10.2217	28.7406	3.0871	13.1142
	% error	0.4412	0.4770	0.0356	0.0869

Table 4
Non-dimensional transverse frequencies ($\omega = \mu L^2 \sqrt{\rho A_0/E_0 I_0}$) for linearly tapered AFG beam ($E(\xi) = E_0 e^\xi$, $\rho(\xi) = \rho_0 e^\xi$).

α	Research work by	Vibration frequencies			
		CC		CF	
		ω_1	ω_2	ω_1	ω_2
0.1	Present	21.2096	58.3740	2.6057	19.4105
	[36]	21.2898	58.6306	2.6060	19.4129
	% error	0.3767	0.4376	0.0115	0.0123
0.3	Present	18.6771	51.6326	2.7086	18.1005
	[36]	18.7484	51.8608	2.7083	18.1001
	% error	0.3802	0.4400	0.0110	0.0022
0.5	Present	15.9648	44.3712	2.8569	16.6915
	[36]	16.0271	44.5698	2.8563	16.6882
	% error	0.3887	0.4456	0.0210	0.0197
0.8	Present	11.2155	31.5306	3.2930	14.3706
	[36]	11.2653	31.6911	3.2923	14.3621
	% error	0.4420	0.5064	0.0212	0.0591

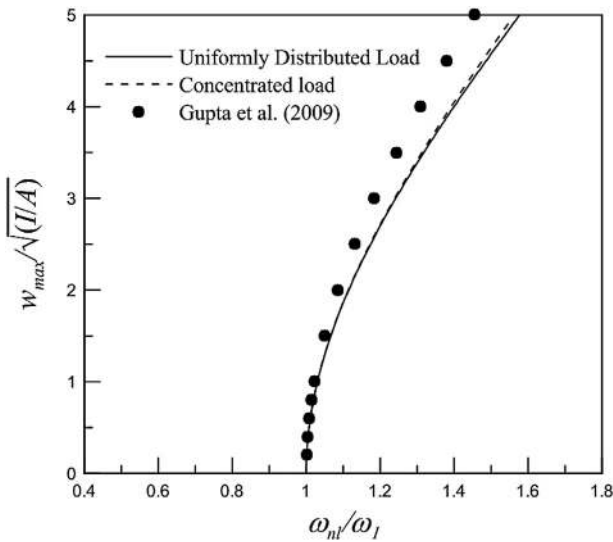


Fig. 4. Comparison of backbone curves for fundamental mode of a clamped-clamped homogeneous uniform beam.

Table 5
Values of fundamental frequencies (ω_1) used for the normalisation of vibration frequencies (ω_{nl}).

		Fundamental frequency, ω_1					
		Material 1		Material 2		Material 3	
		$E(\xi) = E_0$		$E(\xi) = E_0(1 + \xi)$		$E(\xi) = E_0 e^\xi$	
		$\rho(\xi) = \rho_0$		$\rho(\xi) = \rho_0(1 + \xi + \xi^2)$		$\rho(\xi) = \rho_0 e^\xi$	
Taper Pattern	Taper parameter	CC	CF	CC	CF	CC	CF
Linear Taper	0.0	22.2898	3.5155	20.3949	2.4254	22.4279	2.5650
	0.2	20.0032	3.6084	18.1479	2.5053	19.9613	2.6530
	0.4	17.5691	3.7378	15.7673	2.6162	17.3489	2.7752
	0.6	14.9037	3.9356	13.1765	2.7846	14.5067	2.9606
Parabolic taper	0.0	22.2898	3.5155	20.3949	2.4254	22.4279	2.5650
	0.2	20.3605	3.7076	18.4750	2.5715	20.3181	2.7207
	0.4	18.2812	3.9521	16.4230	2.7594	18.0664	2.9207
Exponential taper	0.000000	22.2898	3.5155	20.3949	2.4254	22.4279	2.5650
	0.223144	19.4723	3.3856	17.6874	2.3506	19.4575	2.4901
	0.510826	16.3903	3.1905	14.7503	2.2336	16.2349	2.3719
	0.916291	12.8908	2.8743	11.4556	2.0357	12.6189	2.1704

$$[K_{12}] = 0,$$

$$[K_{21}] = \frac{1}{2L^2} \sum_{j=nw+1}^{nw+nu} \sum_{i=1}^{nw} \int_0^1 \left(\sum_{i=1}^{nw} c_i \frac{d\phi_i}{d\xi} \right)^2 \frac{d\phi_i}{d\xi} \frac{d\psi_{j-nw}}{d\xi} E(\xi) A(\xi) d\xi,$$

$$[K_{22}] = \frac{1}{L} \sum_{j=nw+1}^{nw+nu} \sum_{i=nw+1}^{nw+nu} \int_0^1 \frac{d\psi_{i-nw}}{d\xi} \frac{d\psi_{j-nw}}{d\xi} E(\xi) A(\xi) d\xi,$$

$$\{f_{11}\} = L \sum_{j=1}^{nw} \int_0^1 \bar{p}(\xi) \phi_j d\xi, \quad \{f_{12}\} = 0,$$

The governing set of equations for the static analysis is clearly nonlinear in nature, as the stiffness matrix itself is a function of unknown coefficients (c_i).

In the present work, an assumed solution, expressed in terms of finite linear combination of undetermined parameters or coefficients with appropriately chosen functions, is substituted into the suitably obtained energy functionals and the stationary value with respect to the parameters is sought. Substitution of the assumed solution into the governing equations leads to a set of algebraic equations. Since the solution of a continuum problem in general cannot be represented by a finite set of functions, an error (called the residual) is induced when the assumed solution is substituted in the governing equation. The objective is to minimize the residual to find out a set of converged values for the unknown coefficients.

The nonlinear set of governing equations is solved through an iterative direct substitution method, employing an appropriate relaxation technique. For every load step the values of unknown coefficients (c_i) are assumed to evaluate the stiffness matrix. Using this assumed stiffness matrix new values of unknown coefficients are calculated by the matrix inversion technique from the expression; $\{c\} = [K_s]^{-1}\{f\}$. Calculated values are then compared with their values in previous iteration and if the difference is more than the predefined error limit the process is repeated with new values of unknown coefficients modified with a relaxation parameter until the difference becomes less than the error limit. When the convergence is achieved, c_i are known and thus the displacement field for the beam is computed. At the end of the static solution step, a completely known stiffness matrix is

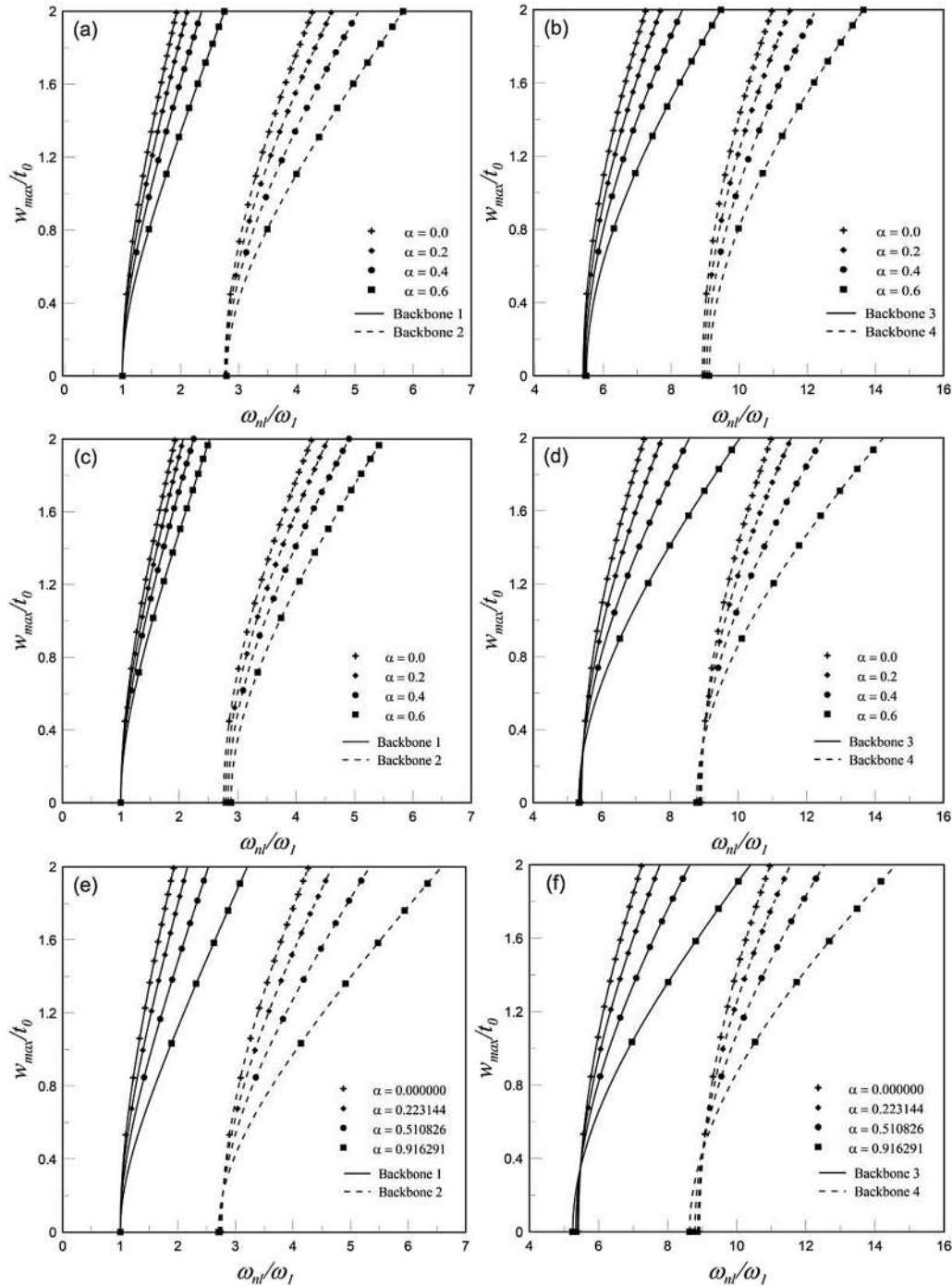


Fig. 5. Backbone curves for AFG beam ($E(\xi) = E_0(1 + \xi)$, $\rho(\xi) = \rho_0(1 + \xi + \xi^2)$): CC (a, b) Linear taper (c, d) Parabolic taper (e, f) Exponential taper.

obtained which corresponds to the deflected configuration of the system.

2.2. Dynamic analysis

The governing equations for the dynamic analysis are obtained by applying Hamilton's principle which is expressed as,

$$\delta \left(\int_{\tau_1}^{\tau_2} (T - U) d\tau \right) = 0 \tag{11}$$

Here, U is the strain energy corresponding to the deflected shape of the beam and T is the total kinetic energy of the system given by the expression,

$$T = \frac{1}{2} \int_0^L \left\{ \left(\frac{\partial W}{\partial \tau} \right)^2 + \left(\frac{\partial u}{\partial \tau} \right)^2 \right\} \rho(x) A(x) dx \tag{12}$$

The unknown dynamic displacements $w(\xi, \tau)$ and $u(\xi, \tau)$ are assumed to be separable in space and time, the spatial part of the fields are approximated by finite linear combination of admissible orthogonal functions identical to those utilized for static analysis,

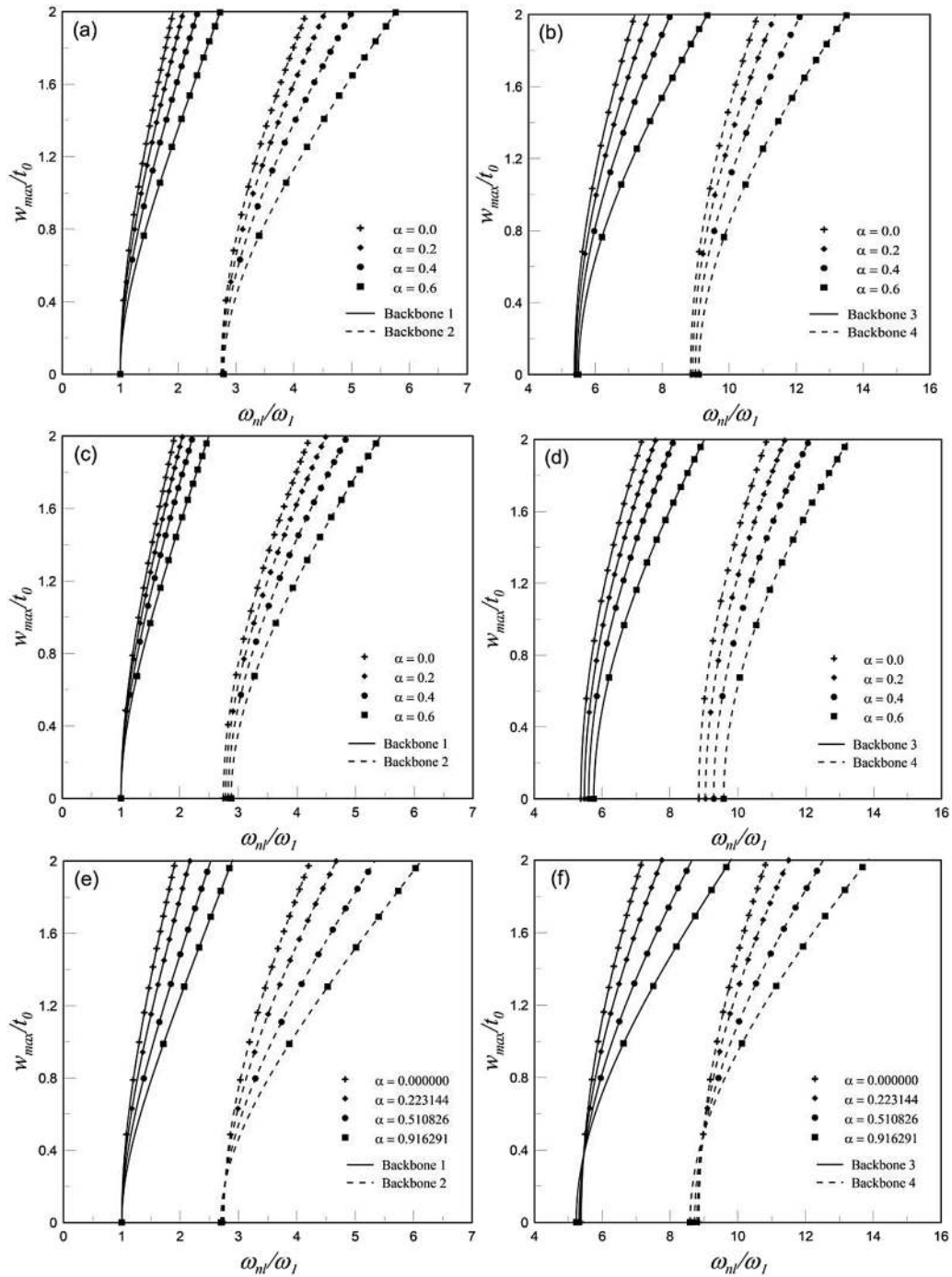


Fig. 6. Backbone curves for AFG beam ($E(\xi) = E_0 e^{\xi}$, $\rho(\xi) = \rho_0 e^{\xi}$): CC (a, b) Linear taper (c, d) Parabolic taper (e, f) Exponential taper.

$$w(\xi, \tau) = \sum_{i=1}^{nw} d_i \phi_i(\xi) e^{j\omega\tau} \text{ and } u(\xi, \tau) = \sum_{i=nw+1}^{nw+nu} d_i \psi_i(\xi) e^{j\omega\tau} \quad (13)$$

where, ω is the natural frequency of the system and d_i represents a new set of unknown coefficients that represents the eigenvectors in matrix form. Substituting Equations (3) and (12) along with the dynamic displacement fields in Equation (11) gives the governing set of equations for the beam in the following form,

$$-\omega^2 [M] \{d\} + [K] \{d\} = 0 \quad (14)$$

where, $[M]$ is mass matrix, which has the following form and elements:

$$[M] = \begin{bmatrix} M_{11} & M_{12} \\ M_{21} & M_{22} \end{bmatrix}$$

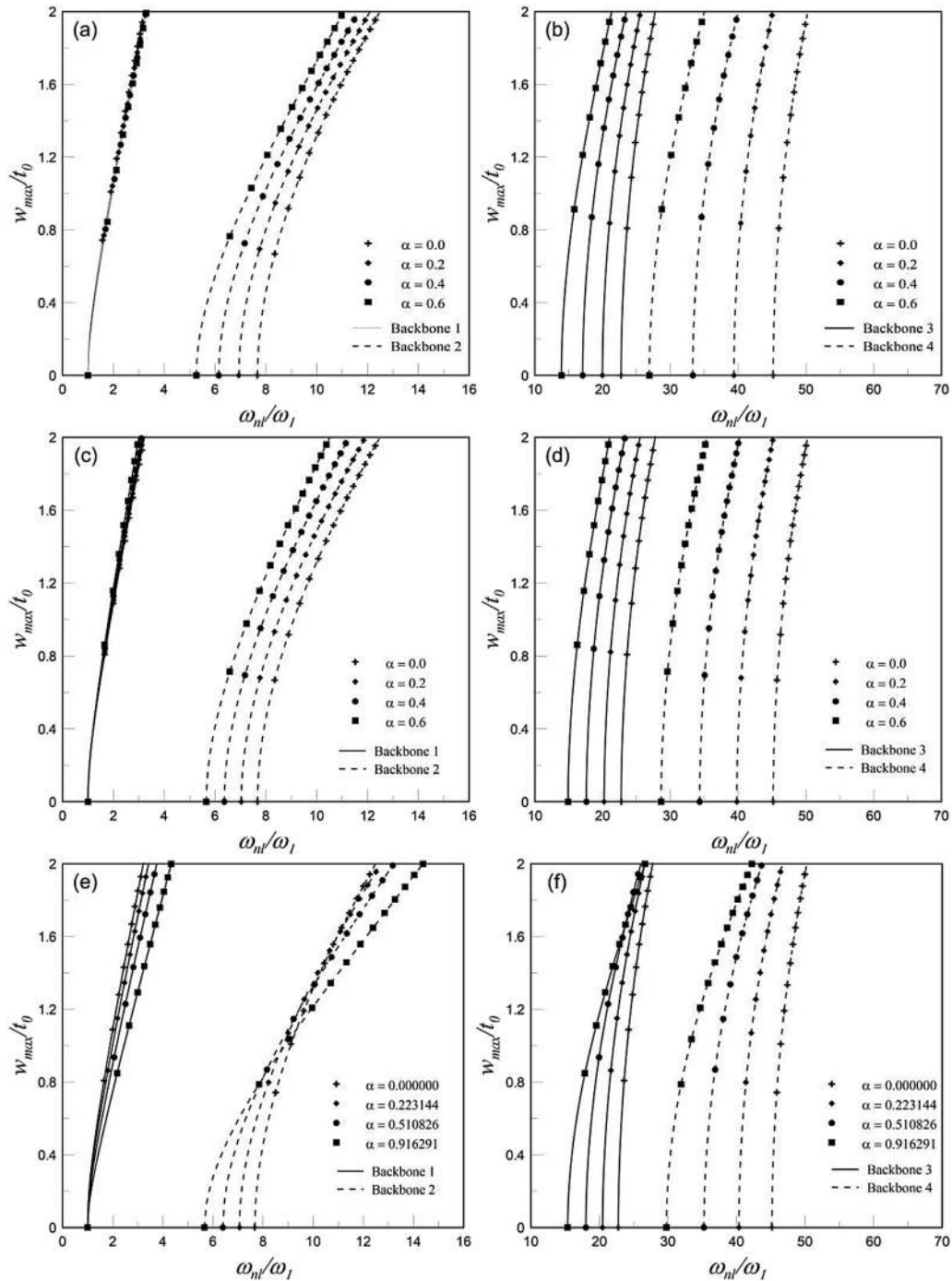


Fig. 7. Backbone curves for AFG beam ($E(\xi) = E_0(1 + \xi)$, $\rho(\xi) = \rho_0(1 + \xi + \xi^2)$): CF (a, b) Linear taper (c, d) Parabolic taper (e, f) Exponential taper.

$$[M_{11}] = L \sum_{j=1}^{nw} \sum_{i=1}^{nw} \int_0^1 \phi_i \phi_j \rho(\xi) A(\xi) d\xi, [M_{12}] = 0, [M_{21}] = 0,$$

$$[M_{22}] = L \sum_{j=nw+1}^{nw+nu} \sum_{i=nw+1}^{nw+nu} \int_0^1 \psi_{i-nw} \psi_{j-nw} \rho(\xi) A(\xi) d\xi,$$

Here, $[K]$ is the stiffness matrix of the system at the deflected configuration. The form and elements of the matrix are identical to that described in the static analysis section. The unknown

parameters obtained from the converged static solution are used to compute the values for $[K]$ at the start of dynamic problem. Equation (14) is a standard eigenvalue problem which is solved numerically through a Matlab programme. The square roots of the computed eigenvalues give the free vibration frequencies at the statically deflected configuration of the beam and are called the loaded natural frequencies. These frequencies, when plotted against corresponding deflection amplitude provide the backbone curves for the system. The eigenvectors corresponding to the eigenvalues are extracted from the same subroutine of Matlab programme and post-processed to obtain the mode shapes of the vibrating system.

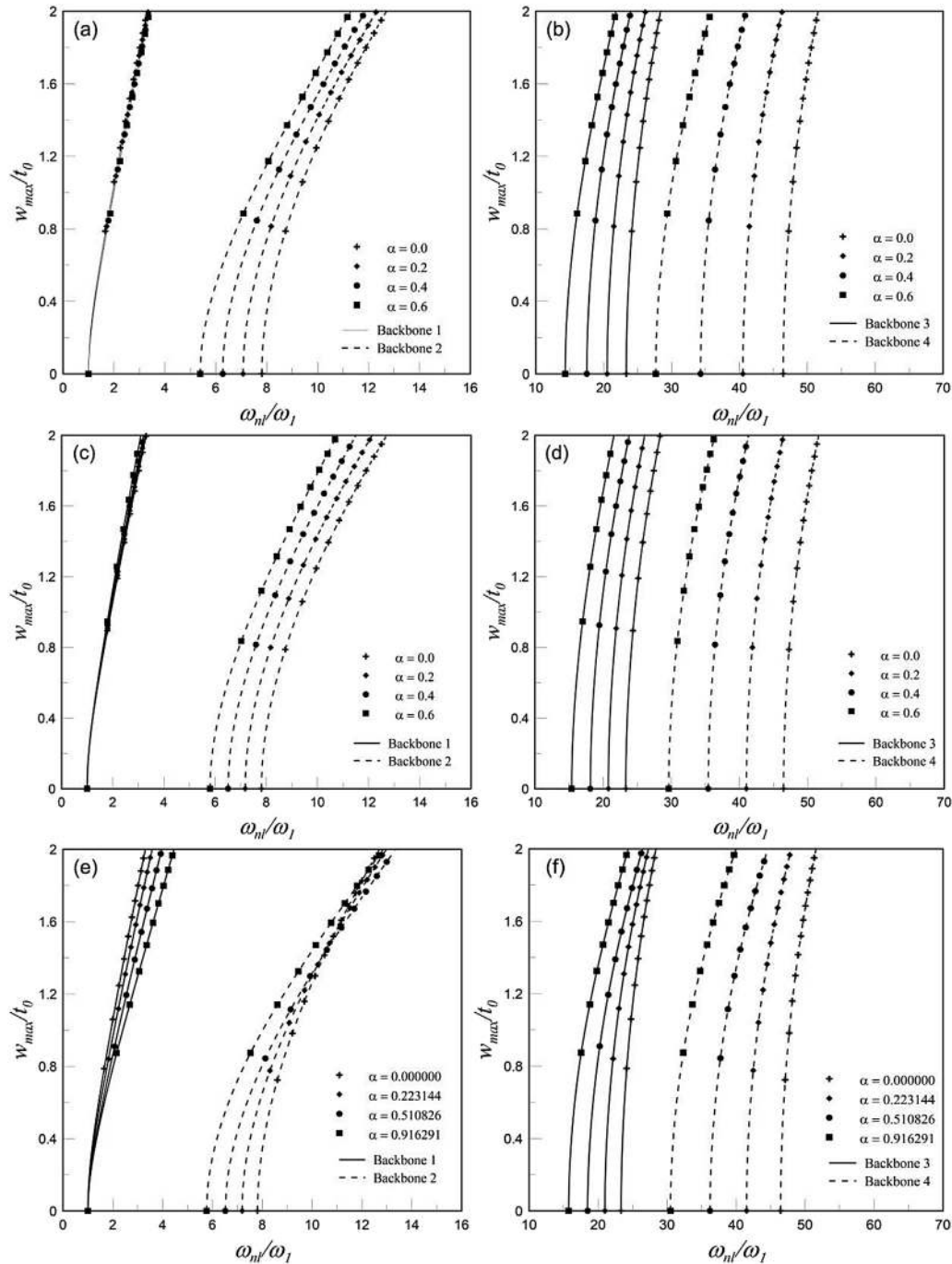


Fig. 8. Backbone curves for AFG beam ($E(\xi) = E_0 e^{\xi}$, $\rho(\xi) = \rho_0 e^{\xi}$): CF (a, b) Linear taper (c, d) Parabolic taper (e, f) Exponential taper.

3. Results and discussions

Present study is conducted with an objective to investigate the effect of large deflection on dynamic behaviour of axially functionally graded (AFG) non-uniform beams and the variations in the said dynamic behaviour corresponding to changes in the taper profile, system geometry and material model. The present analysis is carried out for AFG taper beams under the action of uniformly distributed load for two flexural boundary conditions, namely, Clamped–Clamped (CC) and Clamped-Free (CF). The base functions for the transverse displacements (w) are generated from flexural boundary conditions and that of axial displacements (u) are

generated from membrane boundary conditions. Zero in-plane displacements at the boundaries are assumed for the analysis. These functions are tabulated in Table 1. Gram-Schmidt orthogonalization principle is utilized to generate complete set of higher order functions and the number of functions for each of the displacements is taken as 6. Three such higher order 1-D functions (Mode 2, 3 and 4) corresponding to CC, and CF end conditions are shown in Fig. 2. Due to the general nature of the formulation any other classical flexural boundary conditions can be handled through this method. From combinations of the three classical end conditions, i.e., clamped (C), Simply supported (S) and free (F) ends, a total of 6 different boundary conditions, namely, CC, CS, SS, CF, SF

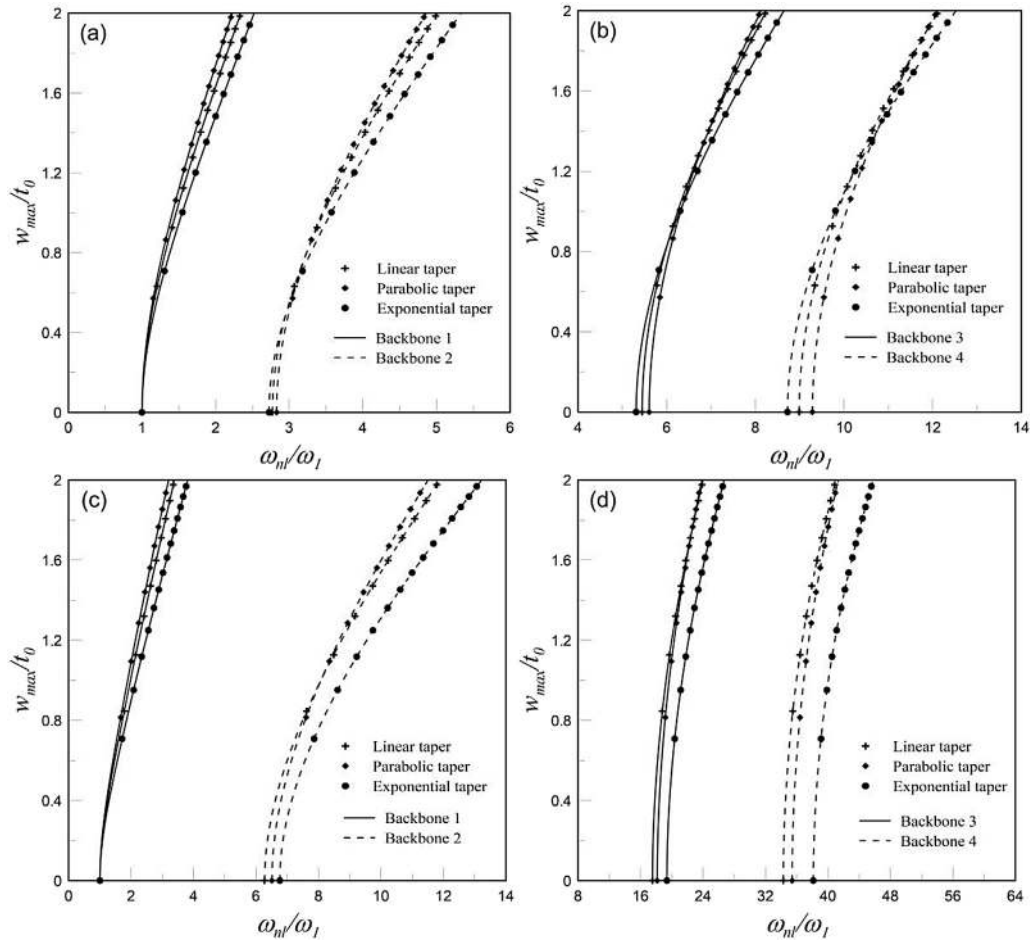


Fig. 9. Comparison of backbone curves for different tapers, $E(\xi) = E_0 e^\xi$, $\rho(\xi) = \rho_0 e^\xi$ (a, b) CC (c, d) CF.

and FF, for a beam can be obtained. Due to the flexible nature of the formulation and solution methodology all these boundary conditions can be efficiently handled as long as proper measures are employed to incorporate the rigid body modes, specifically for SF and FF boundary conditions. Even non-classical boundaries, such as elastically restrained ends, can also be taken care of. However, to limit the volume of the present paper, only results pertaining to CC and CF boundaries are furnished.

Simultaneously, three different taper patterns, namely, linear, parabolic and exponential, have been selected. Schematic representations of the taper profiles considered for the present analysis are shown in Fig. 3 along with their boundary conditions. The beam under consideration is assumed to have uniform width, while the thickness varies according to the relations mentioned in Equation (15).

$$\text{Linear taper : } t(\xi) = t_0(1 - \alpha\xi) \tag{15a}$$

$$\text{Parabolic taper : } t(\xi) = t_0(1 - \alpha\xi^2) \tag{15b}$$

$$\text{Exponential taper : } t(\xi) = t_0 \exp - \alpha\xi^{1/2} \tag{15c}$$

Here t_0 is the thickness of the beam at the root and α is the taper parameter. For each of the taper pattern four different values of taper parameter (α) have been considered and are tabulated in Table 2. The values of α have been so selected that the thickness at

the other end remains same for all the taper patterns to provide a better understanding on the effects of taper pattern on the results.

Three different material models, where, the elastic modulus and density vary along the axial direction, have been considered and the expressions for these two parameters as function of the normalized axial coordinate are given as follows:

$$\text{Material 1: } E(\xi) = E_0, \rho(\xi) = \rho_0 \tag{16a}$$

$$\text{Material 2: } E(\xi) = E_0(1 + \xi), \rho(\xi) = \rho_0(1 + \xi + \xi^2) \tag{16b}$$

$$\text{Material 3: } E(\xi) = E_0 e^\xi, \rho(\xi) = \rho_0 e^\xi \tag{16c}$$

In these expressions, E_0 is the modulus of elasticity and ρ_0 is the mass density at the left end of the beam i.e. at $x = 0$ (Fig. 1). It should be pointed out that *Material 1* refers to a homogeneous material as both elastic modulus and density are constants throughout the beam.

The present analysis is based on a methodology where the solution of the static displacement field of the AFG beam under uniformly distributed transverse loading is obtained, followed by subsequent evaluation of the eigenvalues of the corresponding dynamic problem on the basis of converged static solution. The solution methodology of the static problem involves an iterative numerical scheme using successive relaxation due to presence of nonlinearity in the stiffness matrix. The number of Gauss points (ng) to be used for generation of results is taken as 24. The tolerance

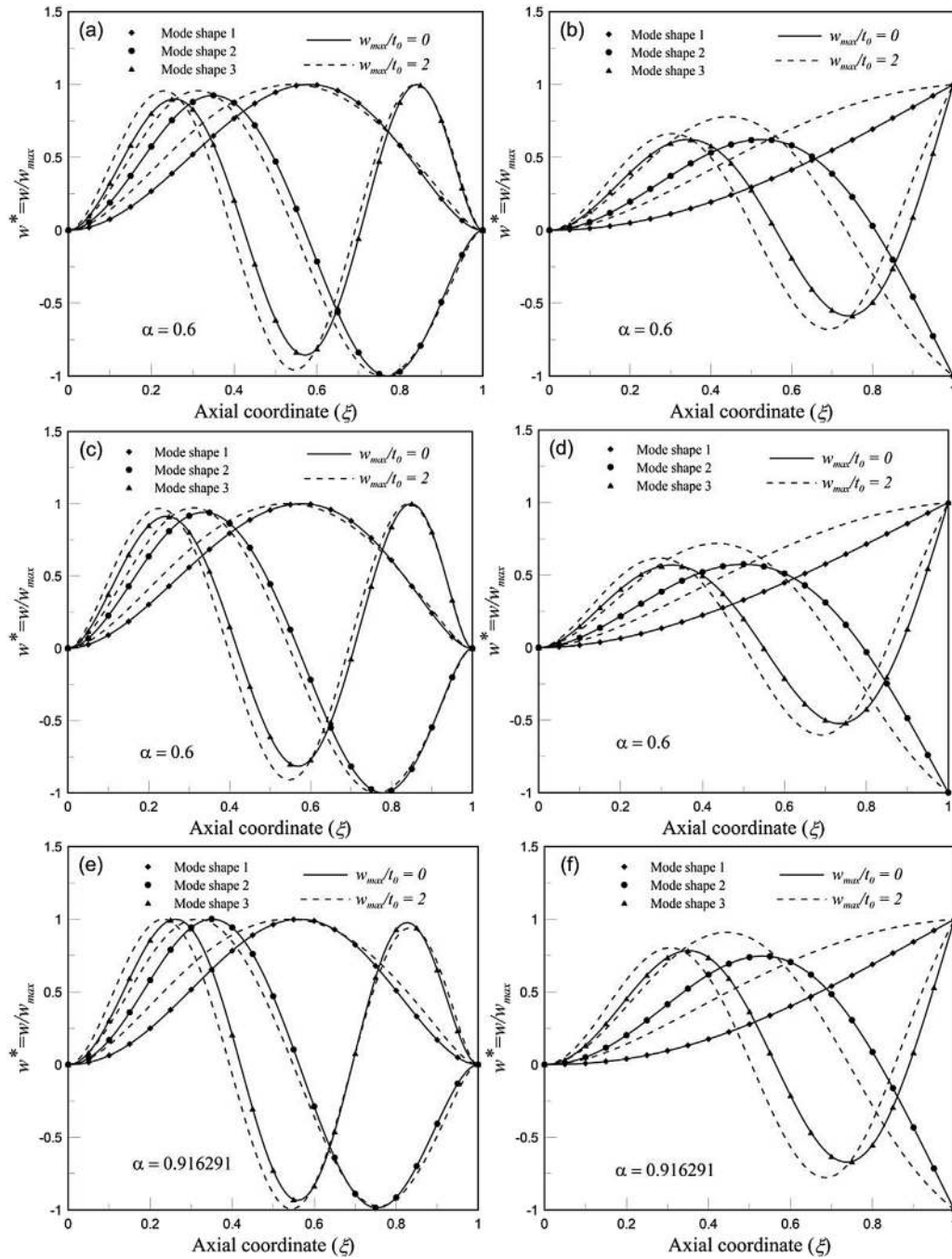


Fig. 10. Mode shape plot for AFG beam ($E(\xi) = E_0(1 + \xi)$, $\rho(\xi) = \rho_0(1 + \xi + \xi^2)$): with Linear taper: (a) CC (b) CF, Parabolic taper: (c) CC (d) CF and Exponential taper: (e) CC (f) CF.

value of the error limit for the numerical iterative scheme is fixed at 0.50% and the relaxation parameter is taken as 0.50. The solution of the dynamic problem is obtained using Matlab subroutines. Following geometrical dimensions and material properties are used to generate the results: $L = 1.0$ m, $b = 0.05$ m, $t_0 = 0.02$ m, $E_0 = 210$ GPa, $\rho_0 = 7850$ kg/m³.

Validation for the present formulation and solution technique is achieved by comparison with established results already available in literature. Non-dimensional free vibration frequency parameters ($\omega = \mu L^2 \sqrt{\rho A_0 / E_0 I_0}$) for different modes of AFG tapered beams are compared with results published by [34] (Table 3) and [36] (Table 4). The tables indicate that the % error between results

obtained from present analysis and published results are quite small and within acceptable limits. The small variations between the two sets of data may be attributed to difference in formulation and solution methodology.

To the best of authors' knowledge, benchmark results for backbone curves or large amplitude free vibration of AFG taper beams are not available in existing literature. Hence, results of the present analysis are validated against a uniform homogeneous beam. Comparative plots for normalized nonlinear frequencies vs normalized maximum deflection corresponding to the fundamental mode are provided in Fig. 4. In this case, present results are compared with results published by [13] for a homogeneous

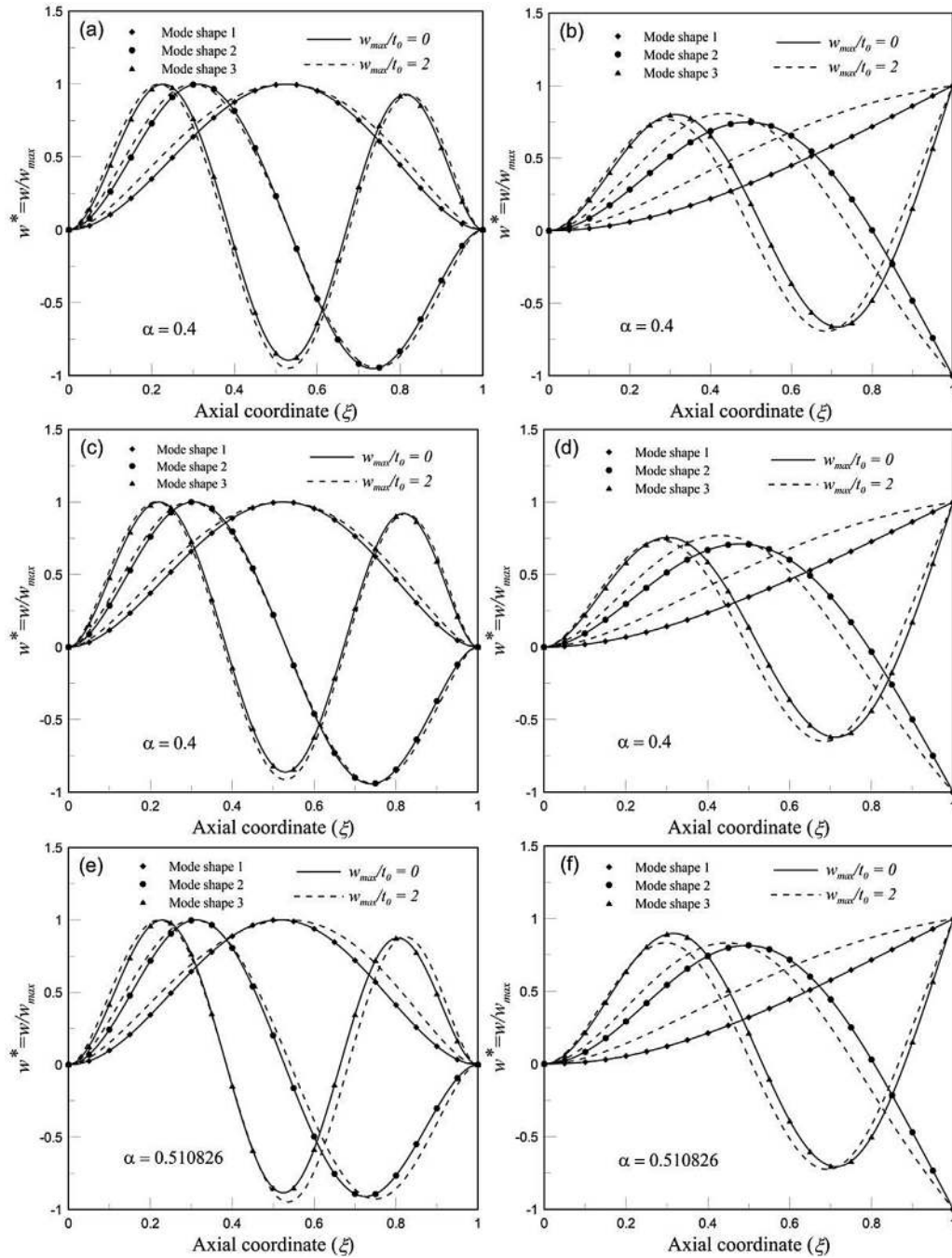


Fig. 11. Mode shape plot for AFG beam ($E(\xi) = E_0e^{\xi}$, $\rho(\xi) = \rho_0e^{\xi}$) with Linear taper: (a) CC (b) CF, Parabolic taper: (c) CC (d) CF and Exponential taper: (e) CC (f) CF.

uniform beam with CC boundary condition. Present results are generated for two different initial deflection profiles corresponding to concentrated and uniformly distributed loading. It is found that the matching of the two sets of results is very good at low load level, but there is some minor deviation at higher loads. However, the trend of the two sets of results is found to be similar. Satisfactory agreement between the existing and generated results is observed throughout all the comparisons to establish the validity of the present formulation and solution methodology.

The fundamental natural frequencies for different conditions are tabulated in Table 5. The effect of various material models, taper patterns and parameters and boundary conditions on free vibration of beams is evident from the differences in frequency parameters. It

is observed that the natural frequencies decrease with increase in taper parameter except for the fundamental mode of linearly and parabolic tapered AFG cantilever beams. This decrease in frequency with the increase in taper parameter is due to the softening effect introduced by the decrease in cross-sectional area and moment of inertia. Similar observations are made by [34] for linearly tapered beams. This softening effect is seen to be most severe in exponentially tapered beams and least on parabolic tapered beams. It is also observed that the natural frequency values for Material 2 are less than those for Material 1 for similar conditions, despite the fact that Material 2 is stiffer than Material 1. However, it should be noted that increasing material properties results in heavier beams and since the natural frequencies are affected by both stiffness and

mass, the variation of natural frequencies with material property variation cannot be easily predicted [35].

Backbone curves of a system provide information about the relation between natural frequency of vibration and amplitude of vibration. It gives a measure of amplitude dependence of the frequency, which happens only for nonlinear systems. Also, idea about the type of nonlinearity (whether hardening/stiffening or softening type) can be obtained from these curves. The large amplitude dynamic behaviour of the system is shown graphically as backbone curves for the first four modes in non-dimensional frequency amplitude plane, where the ordinate and abscissa represent dimensionless amplitude (w_{max}/t_0) and normalized frequency (ω_{nl}/ω_1), respectively. The dimensionless amplitude is the ratio of maximum deflection (w_{max}) to the root thickness (t_0) of the beam whereas the dimensionless frequency is obtained by dividing the nonlinear frequencies (ω_{nl}) by the fundamental linear frequency (ω_1) listed in Table 5. The maximum value of dimensionless amplitude (w_{max}/t_0) is taken as 2.0 for all the cases.

Figs. 5–8 presents the backbone curves for axially FG tapered beams under uniformly distributed transverse loading for different combinations of taper patterns, material property variations, as well as boundary conditions. Each of the figures has three sets of plots (corresponding to three separate taper profiles) containing the first four backbone curves.

Also the figures contain backbone curves for four different values of the taper parameter (α). Figs. 5 and 6 show the backbone curves for clamped (CC) AFG beams having axial gradation according to Material 2 and 3, respectively. Similarly, Figs. 7 and 8 depict the backbone curves for cantilever (CF) AFG beams having axial gradation according to Material 2 and 3, respectively. For all the cases, stiffness of the beam increases with increasing load due to geometric nonlinearity present in the system. This increased stiffness causes the increase in free vibration frequencies with increase in the deflection of the beam, as can be observed from any of the figures. So, hardening type nonlinear behaviour is exhibited by the system for all combinations of taper profile, system geometry, material model and boundary conditions.

For CC boundary conditions (Figs. 5 and 6) individual graphs show an increase in slope of backbone curves with the increase in taper parameter. This is indicative of the fact that nonlinearity of the system increases with increase in taper parameter. The effect of taper parameter is found to be more severe in case of exponentially tapered beams. The backbone curves are comparatively closely clustered in the non-dimensional plane for parabolic taper beams. In case of CF boundary condition (Figs. 7 and 8) it is evident from the figures that the taper parameter does not have much of an effect on the vibration frequencies for the fundamental mode of linearly and parabolic tapered AFG beams and the backbone curves overlap each other.

The variations in the backbone curves with different taper patterns corresponding to Material 3 ($E(\xi) = E_0 e^{\xi}$, $\rho(\xi) = \rho_0 e^{\xi}$) and CC and CF boundary condition are shown in Fig. 9. For this particular case, the taper parameter is kept fixed at 0.4. Nonlinearity involved for exponentially tapered beams is seen to be greater than the other two cases. Difference between the backbone curves for linear and parabolic taper profiles is found to be small.

Mode shape plots for the first three modes are furnished for various taper profile and material property variations to highlight the effect of vibration amplitude on the dynamic behaviour in greater detail (Figs. 10 and 11). For each mode of vibration, two mode shape plots corresponding to linear ($w_{max}/t_0 = 0$) and nonlinear ($w_{max}/t_0 = 2$) frequencies are given. It should also be noted that the amplitude of vibration for all the plots is normalized by the corresponding maximum deflection. As expected the degree of nonlinearity is affected by deflection and is apparent from the

change in particular mode shape. It was also observed that difference in linear and nonlinear mode shapes increase when the boundary condition changes from CC to CF, due to the decreasing rigidity at the boundary. However no considerable change in the mode shapes could be identified by the different taper patterns and material property variations.

4. Conclusions

In the present study, large amplitude free vibration problem of axially functionally graded slender non-uniform beam with various taper profiles and material gradation is investigated. The beam is under the action of uniformly distributed transverse load, while two different flexural boundary conditions (CC and CF) are considered. However the method can be applied to other boundary conditions as well. The mathematical formulation is based on energy method and the free vibration problem is solved in two parts. First the static problem is solved for unknown static displacement fields and subsequently the dynamic problem is taken up based on those known displacement fields. Static analysis is based on principle of minimum total potential energy whereas Hamilton's principle is applied for the dynamic analysis. The methodology is general in nature and can be applied to any type of taper pattern and axial material property gradation, as long as they are expressible in terms of mathematical functions. The results obtained from the present analysis are validated with the previously published results and were found to be in good agreement. Backbone curves are presented in non-dimensional frequency–amplitude plane, whereas mode shape plots are furnished for a few particular cases.

References

- [1] S. Agarwal, A. Chakraborty, S. Gopalakrishnan, Large deformation analysis for anisotropic and inhomogeneous beams using exact linear static solutions, *Compos. Struct.* 72 (2006) 91–104.
- [2] B. Akgoz, O. Civalek, Buckling analysis of linearly tapered micro-columns based on strain gradient elasticity, *Struct. Eng. Mech.* 48 (2) (2013) 195–205.
- [3] B. Akgoz, O. Civalek, Free vibration analysis of axially functionally graded tapered Bernoulli–Euler microbeams based on the modified couple stress theory, *Compos. Struct.* 98 (2013) 314–322.
- [4] A.E. Alshorbagy, M.A. Eltaher, F.F. Mahmoud, Free vibration characteristics of a functionally graded beam by finite element method, *Appl. Math. Model* 35 (2011) 412–425.
- [5] M. Aydogdu, Semi-inverse method for vibration and buckling of axially functionally graded beams, *J. Reinf. Plast. Compos.* 27 (7) (2008) 683–691.
- [6] M. Aydogdu, V. Taksin, Free vibration analysis of functionally graded beams with simply supported edges, *Mater. Des.* 28 (2007) 1651–1656.
- [7] A. Chakraborty, S. Gopalakrishnan, J.N. Reddy, A new beam finite element for the analysis of functionally graded materials, *Int. J. Mech. Sci.* 45 (2003) 519–539.
- [8] S.H. Crandall, *Engineering Analysis: A Survey of Numerical Procedures*, McGraw-Hill, New York, U.S.A., 1956.
- [9] I. Elishakoff, Z. Guede, Analytical polynomial solutions for vibrating axially graded beams, *Mech. Adv. Mater. Struct.* 11 (2004) 517–533.
- [10] A. Fallah, M.M. Aghdam, Nonlinear free vibration and post-buckling analysis of functionally graded beams on nonlinear elastic foundation, *Euro. J. Mech. A/ Solids* 30 (2011) 571–583.
- [11] G. Giunta, D. Crisafulli, S. Belouettar, E. Carrera, Hierarchical theories for the free vibration analysis of functionally graded beams, *Compos. Struct.* 94 (2011) 68–74.
- [12] D.J. Gorman, *Free Vibrations of Beams and Shafts*, Wiley, New York, 1975.
- [13] R.K. Gupta, G.J. Babu, G.R. Janardhan, G.V. Rao, Relatively simple finite element formulation for the large amplitude free vibrations of uniform beams, *Fin. El. Anal. Des.* 45 (2009) 624–631.
- [14] H. Hein, L. Feklistova, Free vibrations of non-uniform and axially functionally graded beams using Haar wavelets, *Eng. Struct.* 33 (2011) 3696–3701.
- [15] M. Hemmatnezhad, R. Ansari, G.H. Rahimi, Large-amplitude free vibrations of functionally graded beams by means of a finite element formulation, *Appl. Math. Model* 37 (2013) 8495–8504.
- [16] Y. Huang, X.-F. Li, A new approach for free vibration of axially functionally graded beams with non-uniform cross-section, *J. Sound. Vib.* 329 (2010) 2291–2303.
- [17] Y. Huang, X.-F. Li, Buckling analysis of nonuniform and axially graded columns with varying flexural rigidity, *J. Eng. Mech.* 137 (2011) 73–81.

- [18] Y. Huang, L.-E. Yang, Q.-Z. Luo, Free vibration of axially functionally graded Timoshenko beams with non-uniform cross-section, *Compos. Part B* 45 (2013) 1493–1498.
- [19] A.S. Kanani, H. Niknam, A.R. Ohadi, M.M. Aghdam, Effect of nonlinear elastic foundation on large amplitude free and forced vibration of functionally graded beam, *Compos. Struct.* 115 (2014) 60–68.
- [20] S. Kapuria, M. Bhattacharyya, A.N. Kumar, Bending and free vibration response of layered functionally graded beams: a theoretical model and its experimental validation, *Compos. Struct.* 82 (2008) 390–402.
- [21] L.L. Ke, J. Yang, S. Kitipornchai, An analytical study on the nonlinear vibration of functionally graded beams, *Meccanica* 45 (2010) 743–752.
- [22] N.D. Kien, Large displacement response of tapered cantilever beams made of axially functionally graded material, *Compos. Part B* 55 (2013) 298–305.
- [23] S.K. Lai, J. Harrington, Y. Xiang, K.W. Chow, Accurate analytical perturbation approach for large amplitude vibration of functionally graded beams, *Int. J. Non-Linear Mech.* 47 (2012) 473–480.
- [24] X.-F. Li, A unified approach for analyzing static and dynamic behaviors of functionally graded Timoshenko and Euler–Bernoulli beams, *J. Sound. Vib.* 318 (2008) 1210–1229.
- [25] X.-F. Li, Y.-A. Kang, J.-X. Wu, Exact frequency equations of free vibration of exponentially functionally graded beams, *Appl. Acoust.* 74 (2013) 413–420.
- [26] C.-F. Lu, W.Q. Chen, Free vibration of orthotropic functionally graded beams with various end conditions, *Struct. Eng. Mech.* 20 (4) (2005) 465–476.
- [27] A.J. Mazzei Jr., R.A. Scott, On the effects of non-homogeneous materials on the vibrations and static stability of tapered shafts, *J. Vib. Control* 19 (5) (2012) 771–786.
- [28] A. Mitra, P. Sahoo, K. Saha, Free vibration analysis of initially deflected stiffened plates for various boundary conditions, *J. Vib. Control* 17 (14) (2011) 2131–2157.
- [29] J. Murin, M. Aminbaghai, V. Kutis, Exact solution of the bending vibration problem of FGM beams with variation of material properties, *Eng. Struct.* 32 (2010) 1631–1640.
- [30] T.-K. Nguyen, T.P. Vo, H.-T. Thai, Static and free vibration of axially loaded functionally graded beams based on the first-order shear deformation theory, *Compos. Part B* 55 (2013) 147–157.
- [31] H. Niknam, M.M. Aghdam, A semi analytical approach for large amplitude free vibration and buckling of nonlocal FG beams resting on elastic foundation, *Compos. Struct.* 119 (2015) 452–462.
- [32] M.T. Piovani, R. Sampaio, Vibrations of axially moving flexible beams made of functionally graded materials, *Thin-Wall. Struct.* 46 (2008) 112–121.
- [33] K.K. Pradhan, K. Chakraverty, Free vibration of Euler and Timoshenko functionally graded beams by Rayleigh–Ritz method, *Compos. Part B* 51 (2013) 175–184.
- [34] A. Shahba, S. Rajasekaran, Free vibration and stability of tapered Euler–Bernoulli beams made of axially functionally graded materials, *Appl. Math. Model* 36 (2012) 3094–3111.
- [35] A. Shahba, R. Attarnejad, S. Hajilar, Free vibration and stability of axially functionally graded tapered Euler–Bernoulli beams, *Shock Vib.* 18 (2011) 683–696.
- [36] A. Shahba, R. Attarnejad, S. Hajilar, A mechanical-based solution for axially functionally graded tapered Euler–Bernoulli beams, *Mech. Adv. Mater. Struct.* 20 (2013) 696–707.
- [37] A. Shahba, R. Attarnejad, M. Marvi, S. Hajilar, Free vibration and stability analysis of axially functionally graded tapered Timoshenko beams with classical and non-classical boundary conditions, *Compos. Part B* 42 (2011) 801–808.
- [38] M. Simsek, Fundamental frequency analysis of functionally graded beams by using different higher-order beam theories, *Nucl. Eng. Des.* 240 (2010) 697–705.
- [39] M. Simsek, T. Kocaturk, Free and forced vibration of a functionally graded beam subjected to a concentrated moving harmonic load, *Compos. Struct.* 90 (2009) 465–473.
- [40] M. Simsek, T. Kocaturk, S.D. Akbas, Dynamic behavior of an axially functionally graded beam under action of a moving harmonic load, *Compos. Struct.* 94 (2012) 2358–2364.
- [41] S.A. Sina, H.M. Navazi, H. Haddadpour, An analytical method for free vibration analysis of functionally graded beams, *Mater. Des.* 30 (2009) 741–747.
- [42] H. Su, J.R. Banerjee, C.W. Cheung, Dynamic stiffness formulation and free vibration analysis of functionally graded beams, *Compos. Struct.* 106 (2013) 854–862.
- [43] S. Suresh, A. Mortensen, *Fundamentals of Functionally Graded Materials*, IOM Communications Limited, London, 1998.
- [44] H.-T. Thai, T.P. Vo, Bending and free vibration of functionally graded beams using various higher order shear deformation beam theories, *Int. J. Mech. Sci.* 62 (2012) 57–66.
- [45] N. Wattanasakulpong, B.G. Prusty, D.W. Kelly, M. Hoffman, Free vibration analysis of layered functionally graded beams with experimental validation, *Mater. Des.* 36 (2012) 182–190.
- [46] L. Wu, Q. Wang, I. Elishakoff, Semi-inverse method for axially functionally graded beams with an Anti-symmetric vibration mode, *J. Sound. Vib.* 284 (2005) 1190–1202.
- [47] H. Yaghoobi, M. Torabi, Post-buckling and nonlinear free vibration analysis of geometrically imperfect functionally graded beams resting on nonlinear elastic foundation, *Appl. Math. Model* 37 (2013) 8324–8340.